

Thermal conductivity of condensed D-T and T₂

G. W. Collins

Department of Physics, Ohio State University, Columbus, Ohio 43210

P. C. Souers, E. M. Fearon, E. R. Mapoles, and R. T. Tsugawa

Department of Chemistry and Materials Science, Lawrence Livermore National Laboratory, Livermore, California 94550

J. R. Gaines

Department of Physics, University of Hawaii, Honolulu, Hawaii 96822

(Received 27 June 1988; revised manuscript received 11 September 1989)

The thermal conductivity of condensed T₂ and D-T has been measured by conventional techniques. Measurements for solid T₂ and D-T (D₂-DT-T₂) from the triple points to 3 K are presented, along with measurements in the liquid phases from the triple points to 25 K. The sample geometry was that of a thin disk, a single heater being used to produce a temperature difference between the faces of the disk. The steady-state thermal conductivity of the solid increases from 0.15 W/m K at 3 K to between 0.5 and 0.7 W/m K at 8 to 10 K before dropping to 0.3 W/m K at the triple points. Two T₂ samples had large thermal conductivities (≈ 1.2 W/m K) at 9 K, probably caused by accidentally good sample packing. The liquid thermal conductivity increases from 0.3 W/m K at the triple points to between 2 and 6 W/m K at 25 K, with convection of the liquid being probable. The effect of shrinkage upon freezing is considered, and an unexplained time-dependent behavior, seen in both T₂ and D-T, is described. The considerable importance of the solid thermal conductivity to nuclear spin polarization of D-T is discussed in detail. The need for a triton spin-lattice-relaxation time greater than 100 s is made evident by the need to remove the heat due to tritium decay and that from microwave pumping of the electron spins.

I. INTRODUCTION

Achievement of near-total parallel alignment of both deuteron nuclear spins and triton nuclear spins in solid deuterium tritide (nuclear spin polarization) would have interesting scientific and technological consequences. The technological interest is related to the possible use of D-T as a target material for nuclear fusion. Kulsrud *et al.*¹ have predicted that the cross section for hydrogen fusion for spin-polarized samples will increase by 50% over that for samples with the random magnetic mix. More² calculated that the initial nuclear spin polarization would not be destroyed by the laser shot in inertial-confinement fusion (ICF). Pan and Hatchett³ then estimated that the laser driver could be reduced to half the normal size if nuclear-spin polarized fuel was used.

The scientific interest comes from numerous studies of other highly polarized spin systems coupled with frustration over the lack of success in producing large polarizations of the nuclear spins in any solid hydrogen sample. Polarized targets based on more complicated spin systems have been used for years in high energy physics experiments. Protons (which have almost the same size magnetic moment as tritons) have been polarized in Cr(V)-doped 1,2-propanediol to between 98 and 100% by deBoer and Niinikoski.⁴ Deuterons have proven to be much harder to polarize than protons. Using deuterated solid ammonia, Meyer *et al.*⁵ have achieved a vector polarization of 44%. This degree of polarization is inadequate

for fusion requirements, although solid ammonia is currently the best of all known candidates. The nuclear spin-lattice-relaxation times (T_1) of the materials above are all over 10^4 s. To achieve such long relaxation times, temperatures as low as 0.3 K have been required. The time constant T_1 can be thought of as the nuclear spin polarization "memory time." For successful polarization, it should be as long as possible.

Although much work has been done on polarizing protons and deuterons in various substances, the only viable fusion fuel is deuterium-tritium. This is because D-T has the largest fusion cross section⁶ and as a fuel will have no nonfusible nuclei. When condensed into the liquid or solid phase, the fuel density could be greatly increased. Unfortunately, the intrinsic tritium radioactivity creates many problems for potential spin polarization.⁷ First, self-heating from a heat flux of 200 mW/g,⁸ coupled with an unknown Kapitza boundary resistance for the samples, apparently precludes cooling to millikelvin temperatures in a large static magnetic field where brute-force nuclear polarization is possible. Because of the higher working temperatures dictated by the tritium self-heating, we earlier suggested that dynamic nuclear polarization (DNP), the method used for nearly all nuclear targets, be used instead.⁷ A second problem caused by the tritium is that the radiation created equilibrium of 25% D₂-50% DT-25% T₂ in equimolar D-T leads to a steady state *o*-T₂ concentration of a few percent that drastically shortens the nuclear T_1 's. This mixture at 3

to 6 K has as its shortest spin-lattice-relaxation time, that of the triton, a value of only 0.3 s. By analogy with solid hydrogen deuteride, we suggested that ultrapure molecular DT would be the desired, long-time constant species of interest.⁷ We have succeeded in making D-T with up to 95% mol% of DT and by doping such samples with *n*-H₂, we have obtained relaxation times of 6 to 8 s.⁹

Since it will be necessary to remove the heat put into the sample in the DNP process from the microwave pump as well as the heat coming from the radioactive decay, the thermal conductivity of solid DT is a critical property. We have previously estimated the thermal conductivity from NMR data we obtained on solid T₂,¹⁰ but the first direct measurements are given here. In this paper, in addition to the direct measurements of the thermal conductivity of T₂, H₂, and D-T, we discuss the implications of the magnitude of the conductivity on successful DNP experiments.

II. EQUIPMENT AND PROCEDURE

The sample cell was made of two oxygen-free copper sections. The cell has an inner radius of 9.5 mm and height of 1.32±0.05 mm. The height was determined after final assembly by x-ray radiography and confirmed by measurement of the resulting photographs. The two copper cell sections were connected by a stainless steel tube of wall thickness 75±12 μm. Germanium resistance thermometers, greased for high thermal conductivity, were varnished into the top and bottom copper sections. The stainless steel fill line has an inner diameter of 1.0 mm and was in thermal contact with the upper copper section before reaching the cell. The heater was wound on tape and varnished to the bottom copper section. The cylindrical cell was threaded into the cold block of an Airco helium flow cryostat (1 W cooling power). A pump with 26 ft³/min capacity was used to produce temperatures below 4.2 K. The thermal conductivity was obtained by measuring the temperature difference between the top and bottom faces of a disk shaped sample. The two faces of the sample must be in good contact with both the upper and lower copper sections of the cell as it is the temperature difference between them that is used to compute the thermal conductivity. We neglect any contributions to the temperature difference due to solid to solid boundary resistance.

The quasi-one-dimensional geometry made it easy to use the classical temperature gradient method to determine the thermal conductivity. We assumed the thermal conductivity was temperature independent and solved the heat conduction equation.¹¹

$$K \frac{dT}{dz} = A_0 z + \frac{H}{A} . \quad (1)$$

Here, K is the thermal conductivity (W/m K), T the temperature (K), z the sample position coordinate (m), A_0 the tritium self-heating (W/m³), H the bottom heater power (W), and A the cross-sectional area (equal to 2.835×10⁻⁴ m²). Equation (1) can be integrated from 0 to L (the sample thickness) to give the temperature

difference across the sample, ΔT ;

$$\Delta T = \frac{L}{K} \left[\frac{A_0 L}{2} + \frac{H}{A} \right] . \quad (2)$$

The directly measured quantity is ΔT and K is calculated from

$$K = \frac{L}{\Delta T} \left[\frac{A_0 L}{2} + \frac{H}{A} \right] . \quad (3)$$

The mean sample temperature, $\langle T \rangle$, can be expressed as

$$\langle T \rangle = \frac{1}{L} \int_0^L T(z) dz = T_0 + \frac{L}{2K} \left[\frac{A_0 L}{3} + \frac{H}{A} \right] , \quad (4)$$

where T_0 is the temperature of the bottom face of the top copper block. The tritium self-heating term can be expressed as

$$A_0 = (1.954) f_T \rho , \quad (5)$$

where f_T is the atomic fraction of tritium in the sample and ρ is the density (mol/m³) of the sample. For the solid, we estimate the density from the equation

$$\rho_s(T) = [V_s(0) + AT^b]^{-1} . \quad (6)$$

For *n*-H₂, D-T and T₂, we use the values $V_s(0) = 22.76$, 19.29, and 18.78×10⁻⁶ m³/mol; with $A = 2.233$, 1.680, and 1.571×10⁻¹² m³/mol K^{*b*}; and $b = 4.424$, 4.276, and 4.242, respectively.¹² These values are suitable from near 0 K to the triple points. The numbers for D-T and T₂ have not been measured but are estimated from data on the other solid hydrogens.

The liquid densities are given by

$$\rho_L = A - BT^2 . \quad (7)$$

For D-T and T₂, the constants are $A = 49\,290$ and 51 100 mol/m³; and $B = 12.90$ and 13.54 mol/m³ K².¹³ No data have been taken for D-T.

One crucial issue for all thermal conductivity measurements in the solid hydrogens is the following: At the triple point, the volume shrinks (about 12%) upon freezing and also decreases a small amount from the triple point to 4 K (about 2 to 3%). Our samples are loaded into the cell as liquids and then frozen. A slow freeze taking over half an hour was used. Just at the freezing point, heat pulses are applied to the fill line so that the more liquid can trickle into the cell but the actual fill density of the solid hydrogen is unknown. There is also the possibility that shrinkage may produce a crack between the hydrogen and one of the copper plates. This situation is not unique to our experiments but exists in all previous measurements of the thermal conductivity of solid H₂ and D₂ made under the saturated vapor pressure.¹⁴⁻¹⁷ While large thermal conductivities have been measured, Bohn¹⁸ has concluded that there is no way to judge the solid-filling problem in any of the work presently in the literature. The only way to assure complete filling would be to apply pressures as high as 12 MPa for D-T and 14 MPa for T₂.¹⁹ These pressures would assure complete cell filling even to 0 K. H. Meyer has pressurized H₂ to 10

MPa (twice the expected pressure) in order to ensure good plate contact for dielectric constant measurements.²⁰ This difficult technique has been extended to thermal conductivity measurements in the work of Calkins and Meyer.²¹

Another experimental problem comes from the heat conducted by the stainless steel walls of the sample cell. For H₂, Mylar may be used,²² providing thermally insulating walls, but fear of losing the tritium sample dictated the use of metal for the walls, hence the choice of thin-wall stainless steel. The steel has a thermal conductivity comparable to that of the hydrogen (about 0.3 to 0.5 W/m K,²³ but the cross-sectional area of the steel is only 1.6% that of the hydrogen. Thus if the hydrogen is in good contact with the copper, the heat conducted by the steel walls is a small effect that can be corrected for.

Since our method relies on the steady-state temperature difference between two plates (ΔT), we must know the time constant characteristic of the system's thermal response. The appropriate time constant τ is²⁴

$$\tau = \left[\frac{2L}{\pi} \right]^2 \left[\frac{C\rho_s}{K} \right], \quad (8)$$

where L is the thickness of the material under consideration, C the heat capacity, ρ_s is the density, and K is the thermal conductivity. For the solid hydrogen sample, let us take $K \approx 0.1$ W/m K as the smallest value of K and $C \approx 5$ J/mol K. Then $\tau_{(\text{hydrogen})} \approx 4$ s, where the steel walls have about the same value. The copper, however, has a large thermal conductivity of about 500 W/mol K at 4 K and a heat capacity of about 6 J/mol K.²³ This leads us to time constants of 0.6 and 0.1 s for the upper and lower copper blocks. Whether longer time constants exist due to poorly made connections or other causes was tested by rapidly raising and lowering the temperature of a solid H₂ sample. No such effects were seen.

With our sample cell empty, the bottom copper section was thermally isolated. Its temperature increased precipitously when the bottom heater was turned on, showing the effectiveness of the stainless steel walls as insulation. We next added nearly normal H₂ ($x = 0.65$ – 0.72), where x is the fraction of $J=1$ hydrogen in the entire mixture, for calibration. We found that a temperature difference existed even with the heater off that amounted to a power input of 0.003 ± 0.002 W. This led us to use 0.105 W (which produced $\Delta T \approx 1$ to 3 K) as the standard heater power in this work, a value that is at least twenty times the "background" power. With solid T₂ and no heater, the use of 0 W in Eq. (3) produced erroneous thermal conductivities, twice as large as those seen at 0.105 W, but only in the temperature range of 4 to 9 K, where the thermal conductivity reaches its peak. On the other hand, increasing the heater power to 0.432 W had no effect on the derived thermal conductivity values.

We next compared our results on the H₂ sample with $x = 0.65$ – 0.72 with that of Heubler and Bohn¹⁴ taken at $x = 0.70$. As seen as Fig. 1, the two sets of data are comparable at 6 K where $K \approx 0.3$ W/m K but at the 10 K maximum in the conductivity, we get 0.5 W/m K com-

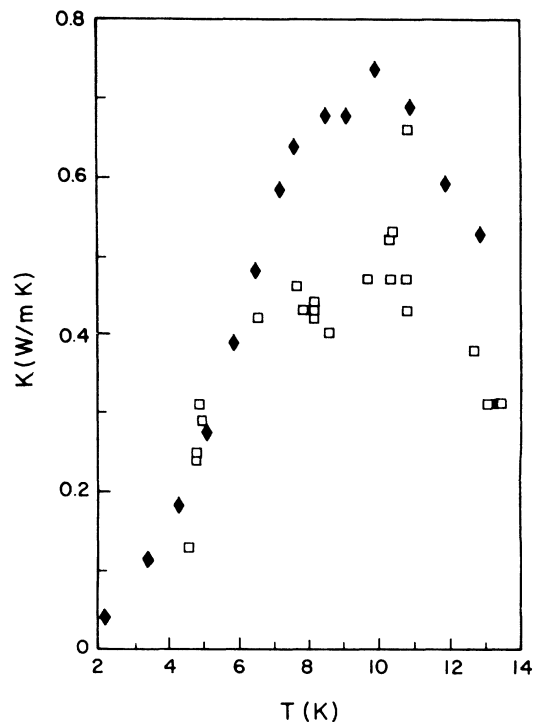


FIG. 1. The thermal conductivity of H₂ with $J=1$ concentration between 72% and 65%, measured in our cell, is compared to the work of Heubler and Bohn (Ref. 14). The symbols are \blacklozenge Heubler and Bohn (70% $J=1$ concentration); \square our calibration for a mean concentration of 68%.

pared with 0.7 W/m K in their work and at 13 K, the values are 0.3 and 0.5 W/m K, respectively. We may speculate as to why our values above 6 K are lower than those of Heubler and Bohn. Their cell was 10 mm in diameter with a height of 500 mm so that it may have been easier to load than ours, resulting in a lower "fill factor" in our case.

The compositions of the tritiated samples were determined by magnetic sector mass spectroscopy and are listed in Table I. The D-T is assumed to have the room temperature equilibrium at cryogenic temperatures.

III. RESULTS AND DISCUSSION

Measurements of the thermal conductivity of solid T₂ at several mean temperatures are shown in Fig. 2 as a function of time. For a given temperature, the thermal

TABLE I. Composition of samples in mol%. The atomic fraction of tritium, f_T , is needed for Eq. (5).

T ₂	HD	0.1	D-T	HD	0.3
	HT	0.5		HT	0.3
	DT	1.0		D ₂	20.0
	T ₂	98.4		DT	45.0
				T ₂	34.4
		100.0			100.0
Atomic T		99.2			57.0
f_T		0.992			0.570

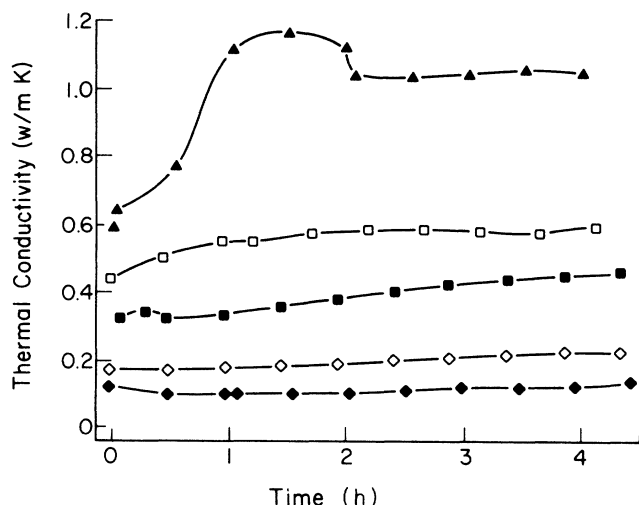


FIG. 2. Thermal conductivity of solid tritium from 3 to 10 K as a function of time. The sensor temperatures are \blacklozenge 3 K; \diamond 4 K; \blacksquare 5 K; \square 10 K; and \blacktriangle 9 K.

conductivity increases slightly with time in most cases. For the two curves at almost the same temperature, the results are very different. The 10 K run is a normal fill, whereas the 9 K data come from an anomalous run. Only two of these occurred in the entire series of experiments, both for solid T₂ between 9 and 10 K. We believe that in the 9 K run, for unknown reasons, the cell “fill factor” was unusually large. The increase in the thermal conductivity with time, for all the samples, is most likely attributed to the radiation-catalyzed reaction of $J=1$ to $J=0$ T₂. It is well known that such catalysis in solid H₂ and D₂ greatly increases the thermal conductivity.^{14–17} The sudden drop in the thermal conductivity for the 9 K sample at two hours could be caused by the sample breaking away from the plates.

To isolate the contribution of the $J=1$ molecules to the thermal conductivity of solid T₂, we calculate the fraction of T₂ in the state $J=1$ from the equation

$$x = (x_0 - x_\infty) \exp\left[-\frac{t}{\tau_J}\right] + x_\infty, \quad (9)$$

where x_0 and x_∞ are the initial and steady-state $J=1$ T₂ concentrations at a given temperature. In the above equation, t is the time and τ_J is the $J=1$ to $J=0$ time constant. The quantities τ_J and x_∞ were previously determined by nuclear magnetic resonance.²⁵ The samples start at $x=0.75$ at room temperature, so that x_0 at the temperature of interest may be calculated using Eq. (9). Typically x_0 is about 0.65.

We next assume that the thermal resistance due to the $J=1$ impurities will be the same in solid T₂ as it is in solid H₂ and D₂. By isolating the contributions in H₂ and D₂ that are due to the $J=1$ impurities only, $K(J=1)$,^{14–17} we can calculate the remaining contribution to the thermal conductivity and extract the thermal resistance $R_{(\text{defect})}$ from

$$R_{(\text{defect})} = \frac{1}{K} - \frac{1}{K(J=1)}. \quad (10)$$

This resistance we attribute to radiation-created defects in the solid T₂. The results of this analysis at four temperatures are shown in Fig. 3. We see that this resistance is both time and temperature dependent. At the higher temperatures, the resistance quickly attains a time-independent value but at the lower temperatures, the time dependence is pronounced and the “long-time” value of the resistance is larger.²⁶ This explains why the time dependence (the $J=1$ dependence) of K is so sluggish in T₂ as compared to that in H₂ or D₂. As the $J=1$ T₂ concentration decreases, it is replaced by defects as the scatterers of phonons.

Additional data were taken for samples with small $J=1$ concentrations. These samples were held at 10 K for four hours since τ_J has its minimum value (0.5 hour) at this temperature as the tritium atoms exercise their maximum catalytic effect at this temperature.^{25,27} After four hours, we expect $x_\infty \approx 0.02$. Moreover, all samples have filled to the normal extent and all time-dependent effects have equilibrated.

The results for solid T₂ and D-T are shown in Fig. 4 for all the samples except the two samples where K was anomalously high. This figure gives the behavior of our typical samples. The shape of the curve is well known from studies of the thermal conductivity of insulators²⁸ and hydrogen in particular. The thermal conductivity increases with temperature at low temperatures as the phonon density increases. When there are a sufficient number of phonons, they interfere with each other (the Umklapp process) and the thermal conductivity decreases with increasing temperature. The fact that D-T is a mixture of three major isotopic constituents apparently causes a decrease in the thermal conductivity as well when compared to T₂. The magnitude of the thermal conductivity of T₂ measured here agrees well with our earlier crude estimate based on NMR experiments.

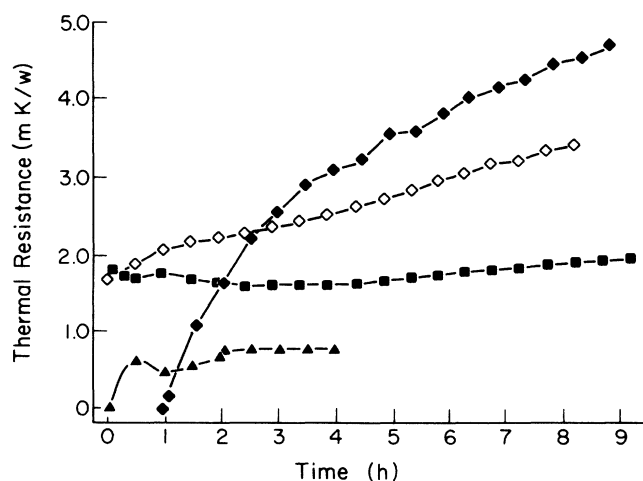


FIG. 3. Calculated defect thermal resistance of solid tritium from 3 to 9 K. The 9 K run is the anomalously high run shown in Fig. 1. \blacklozenge 3 K; \diamond 4 K; \blacksquare 5 K; and \blacktriangle 9 K.

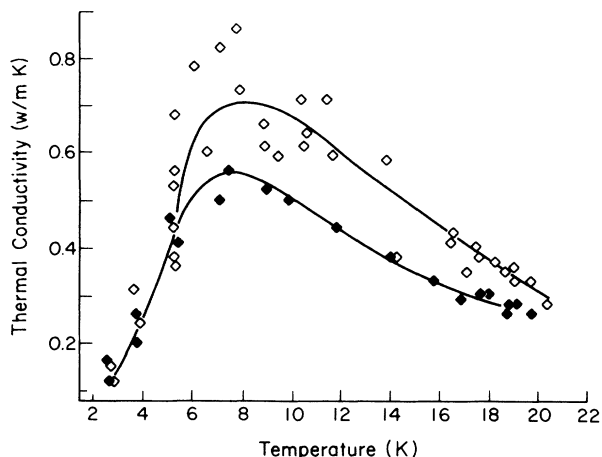


FIG. 4. Steady-state thermal conductivity of solid T_2 and D-T. These points represent a normal filling of the cell with solid. \blacklozenge D-T; \diamond T_2 . The $J=1$ concentration (x) for each point is approximately the dynamic equilibrium concentration for each temperature. For T_2 , at 14.5 K, $x=23.1\%$, at 10 K, $x=5.5\%$, and at 5.3 K, $x=2.9\%$. This quantity was measured in Ref. 25.

To compare the present data with that of solid H_2 , we note that both the temperature where the peak in the thermal conductivity occurs and the magnitude of the conductivity at the peak are very sensitive to the ortho concentration. On the high-temperature side of the peak in H_2 , the thermal conductivity is roughly independent of ortho concentration and equal to 0.5 W/mK, comparable to the value we obtain in T_2 or D-T. At the peak, however, the conductivity of H_2 , for low ortho concentrations, say 2.5%, is 50 W/mK or 50 times larger than we observe. We believe this reduction in conductivity at the peak is most likely due to radiation damage effects in our solids and scattering from the atoms they contain.

The steady-state thermal conductivity of liquid T_2 and D-T is shown in Fig. 5. The liquid data merge with the solid data near the triple point but increase above 24 K. The thermal conductivity of liquid H_2 increases from only 0.10 to 0.12 in the same temperature range,^{29,30} so we are probably observing the results of convection in T_2 and D-T driven by their internal heating. The heater placement on our cell was inadequate for experiments on liquids. To minimize the effects of convection, we *should have* directed the heat current downwards but could not. We have visually observed refluxing of liquid D-T previously in this laboratory.

Additional time-dependent effects were seen with tritiated solids although these effects were not seen for the empty cell nor with solid H_2 . The most dramatic of these effects occurred upon sudden heating from about 3 K to about 5 K. These effects were seen in seven runs out of eight, in both solid T_2 and D-T and are illustrated in Fig. 6 for a T_2 sample first held three hours at 10 K to reduce the $J=1$ concentration. Upon sudden heating from 3.8 to 4.9 K (after 1.2 hours at the lower temperature), the thermal conductivity rose to a large value, then decreased to the steady-state value of Fig. 4. The thermally an-

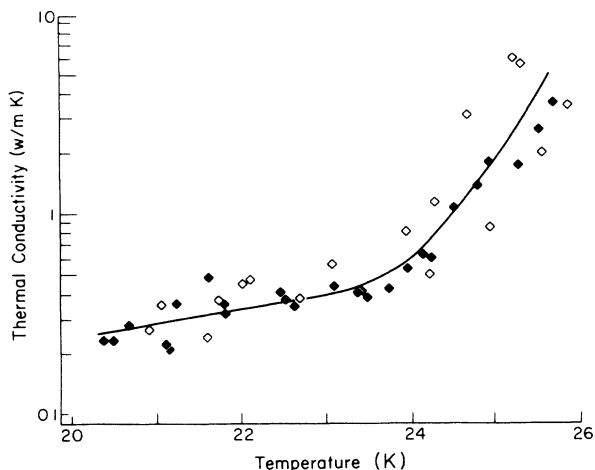


FIG. 5. The thermal conductivity of liquid T_2 and D-T. \blacklozenge D-T; \diamond T_2 .

chored cold upper plate did not change temperature but the thermally floating, hotter, lower plate had its temperature increase steadily.

There are several possible explanations for this phenomenon. One possibility is that the solid touches the walls after the temperature change and then pulls away. This is impossible to rule out but the corresponding effect was not seen, as would be expected, when solid H_2 was used. The most likely explanation is that the large population of hydrogen atoms (previously formed by tritium radioactivity) recombines, releases heat, and temporarily removes scattering centers from the solid improving its thermal conductivity until the atom population is re-established. A larger heat-source term (coming from the

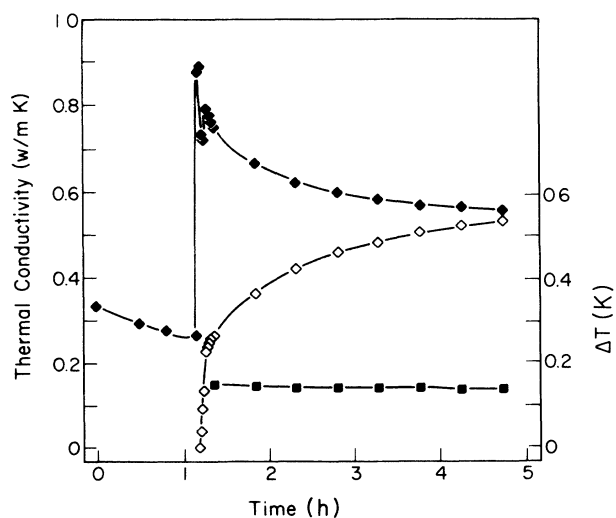


FIG. 6. Time-dependent thermal conductivity (symbol \blacklozenge) seen in solid T_2 upon changing the temperature from 3.8 to 4.9 K at 12 hours. The temperature change from the 1.2 hour point, ΔT , is shown for the hot (symbol \diamond) and cold (symbol \blacksquare) plates as well.

recombination energy) will lower the measured thermal conductivity while removal of "defects" will increase it. The data support this explanation. Initially, after the temperature rise, the enhanced thermal conductivity does show tendencies to decrease (as the recombination heat is taken out) before decaying to its steady-state value. The conductivity at 5 K is roughly 0.35 W/m K. The "defect resistance" was calculated to be 1.6 m K/W. If the observed thermal resistance is the sum of the defect resistance and that of the "pure" crystal, then the conductivity of the crystal, without defects, would be 0.8 W/m K, very close to the observed value.

This explanation is also supported by our recent EPR measurements which show that the atom population is quickly reduced to almost zero following an abrupt temperature increase before it rebuilds. The time constant for reestablishing the atom population gets longer at lower temperatures.

IV. RELATION TO NUCLEAR SPIN POLARIZATION

Now that the thermal conductivity of the major candidate for laser fusion is known, it is possible to discuss the limitations this parameter places on the polarization process. The internal heating of the samples combined with the limitations from the thermal conductivity and the Kapitza resistance dictate that DNP be used. For DNP to be successful, there must be a source of electron spins. In T₂ and DT, the source of electron spins is the tritium β decay that produces atoms. Each β decay produces of the order of 1000 atoms. Because of the constant production of atoms, a dynamic equilibrium population builds up with the number density increasing with decreasing temperature. The mechanism for DNP is discussed below.

The dominant characteristic of the nuclei for DNP is their spin-lattice-relaxation time T₁. This quantity describes how fast the nuclei will forget their polarization (or how long it will take to establish a polarization). Clearly, one criterion for successful polarization is that under irradiation by a microwave pulse, we must achieve the desired polarization in a time t_m where

$$t_m < T_1, \quad (11)$$

where T₁ here refers to the nucleus with the shortest relaxation time, the triton. If P(∞) is the theoretical achievable polarization, then the maximum actual polarization, P(max), will be

$$P(\max) = \frac{P(\infty)}{t_m} \int_0^{t_m} \exp\left[-\frac{t}{T_1}\right] dt, \quad (12)$$

$$\frac{P(\max)}{P(\infty)} = \frac{T_1}{t_m} \left[1 - \exp\left[-\frac{t_m}{T_1}\right] \right]. \quad (13)$$

For t_m ≪ T₁, P(max)/P(∞) approaches unity. Numerically, for the ratio t_m/T₁ = 0.1, 1, or 10, the ratio P(max)/P(∞) = 0.95, 0.63, or 0.10. The highest possible polarization attainable is the initial polarization of the electron spin system. This is given by

$$P(\infty) = \tanh\left[\frac{|\mu_e|B}{kT}\right], \quad (14)$$

where |μ_e| is the absolute value of the electron magnetic moment, B is the dc magnetic field intensity (tesla) and k is the Boltzmann constant.³¹ It is clear from Eq. (14) that if the temperature increases too much, relative to the magnetic field, the electron spin polarization is reduced and any chance for a large nuclear spin polarization is lost.

For simplicity let t_m = T₁. The microwave power density generated in solid D-T, B₀ in W/m³ is given by

$$B_0 = \frac{2N_0 h \nu_e \rho_s}{\epsilon T_1}. \quad (15)$$

Here, N₀ is Avogadro's number, h is Planck's constant, ν_e is the microwave frequency (Hz), and ε is the efficiency of polarization, the number of nuclei polarized per microwave quantum absorbed by the solid. The factor of 2 arises because hydrogen is diatomic. The above term, B₀, represents a "self-heating" term much like the term A₀ used earlier for the tritium radioactive decay, except that B₀ can be much larger than A₀ in a DNP experiment. Equation (14) assumes that all nuclei are available for polarization, i.e., no I=0 molecules are present. We also assume that the polarization time is inherently fast compared to T₁.

There are two distinct mechanisms for DNP with different requirements. Thermal mixing (or dynamic cooling) requires a broad electron-spin-resonance (ESR) line.^{32,33} Here, the free electron distribution is cooled by microwaves and the nuclei can give up their energy to the electrons. The efficiency can be unity at the beginning but it decreases as more and more nuclei become polarized. If all the nuclei are polarized, the solid will continue to absorb microwave energy with zero efficiency.

The second mechanism, the solid-state (or solid) effect, requires a narrow ESR line.^{34,35} In this case, the microwaves drive a double ESR-NMR transition and the electrons deexcite by ESR relaxation. The efficiency is always unity because if all the nuclei are polarized, no double transitions can take place. Despite the high efficiency, there is no guarantee of a large polarization because the double transition is forbidden.

Suppose the efficiency (ε) is unity, ρ_s is 50 000 mol/m³, and ν_e = 94 GHz, then the microwave power density (W/m³) is

$$B_0 \approx \frac{4 \times 10^6}{T_1}. \quad (16)$$

We substitute this into Eq. (2), keeping only the tritium self-heating term to obtain the temperature difference across a sample in a DNP experiment:

$$\Delta T = \frac{(A_0 + B_0)L^2}{2K}. \quad (17)$$

In Table II, we calculate the microwave heating B₀ and the temperature difference across a 1 mm solid D-T sample with a thermal conductivity of 0.1 W/m K (appropri-

TABLE II. Calculated microwave heating in a disk shaped (quasi-one-dimensional) solid D-T sample with a 94 GHz pumping frequency, a thickness of 1 mm, and a thermal conductivity of 0.1 W/m K. The efficiency of nuclear polarization is assumed to be unity.

T_1 (s)	B_0 (W/m ³)	ΔT (K)
10	4×10^5	2.2
100	4×10^4	0.44
1000	4×10^3	0.27

ate for a sample with mean temperature of 2 K). With the longest presently available triton T_1 of about 10 s,¹⁰ even with perfect polarization efficiency, the mean sample temperature will be too high for an acceptable electron spin polarization. For $T_1=1000$ s, the tritium self-heating dominates, and the resulting temperature difference, although large at low temperature, may be bearable.

The results in Table II illustrate how important it is to have a long nuclear relaxation time and considerable effort is going into the attempt to lengthen the triton T_1 . It may also be possible to increase the solid D-T thermal conductivity by compaction of the sample or to design a better D-T to metal bond than now exists. Since we deduce the thermal conductivity from the temperature difference as measured by the temperatures of two copper blocks, a thermal boundary resistance would lead to an

apparently low K . Improvement of the contact would permit utilization of the optimum K . Nuclear target makers routinely cool to low temperatures (0.3 to 0.5 K) in order to lengthen the nuclear relaxation time to days or weeks. There is clearly no point in doing this if the decrease in thermal conductivity more than compensates for the increase in the relaxation time at lower temperatures. Perhaps in the future, superhigh magnetic fields will allow polarization at 8 K, where the D-T thermal conductivity is optimum.

ACKNOWLEDGMENTS

The authors would like to gratefully acknowledge financial support for this work for the Laser Program and the Chemistry and Materials Science (CMS) Department of the Lawrence Livermore National Laboratory and the National Science Foundation (Grant No. DMR 8716520). We wish to thank P. A. Fedders of Washington University for discussions on the efficiency of the mechanisms of DNP. We also wish to thank Chris Gatrousis and Tom Sugihara of the Chemistry and Materials Science Department and Erik Storm of the Inertial Confinement Fusion Program for their support of this work. This work was performed under the auspices of the Department of Energy by Lawrence Livermore National Laboratory under Contract No. W-7405-ENG-48. The work of G.W.C. was performed while under contract to Lawrence Livermore National Laboratory and that of J.R.G. while a consultant to Lawrence Livermore National Laboratory.

¹R. M. Kulsrud, H. P. Furth, E. J. Valeo, and M. Goldhaber, *Phys. Rev. Lett.* **49**, 1248 (1982).

²R. M. More, *Phys. Rev. Lett.* **51**, 396 (1983).

³Y.-L. Pan and S. P. Hatchett, *Nucl. Fusion* **27**, 815 (1987).

⁴W. deBoer and T. O. Niinikoski, *Nucl. Instrum. Methods* **114**, 495 (1974).

⁵W. Meyer, K. H. Ahhoff, W. Havenith, O. Kaul, H. Reichert, E. Schilling, G. Sternal, and W. Thiel, *Nucl. Instrum. Methods* **227**, 35 (1984).

⁶P. C. Souers, *Hydrogen Properties for Fusion Energy* (University of California, Berkeley, 1986), p. 2.

⁷P. C. Souers, E. M. Fearon, E. R. Mapoles, J. R. Gaines, J. D. Sater, and P. A. Fedders, *J. Vac. Sci. Technol. A* **4**, 1118 (1986).

⁸W. L. Pillinger, J. J. Hentges, and J. A. Blair, *Phys. Rev.* **121**, 232 (1961).

⁹P. C. Souers, E. M. Fearon, E. R. Mapoles, J. D. Sater, G. W. Collins, J. R. Gaines, R. H. Sherman, and J. R. Bartlit, *Fusion Tech.* **14**, 855 (1988).

¹⁰J. R. Gaines, R. T. Tsugawa, and P. C. Souers, *Phys. Lett.* **84A**, 139 (1981).

¹¹H. S. Carslow and J. C. Jaeger, *Conduction of Heat in Solids*, second edition (Clarendon, Oxford, 1959), pp. 130–132.

¹²Reference 6, pp. 79–80.

¹³Reference 6, pp. 61–62.

¹⁴J. E. Huebler and R. G. Bohn, *Phys. Rev. B* **17**, 1991 (1978). A detailed list of the unpublished data was kindly sent to us by R. G. Bohn.

¹⁵R. W. Hill and B. Schneidmeyer, *Z. Phys. Chem. Neue Folge* **16**, 257 (1958). From Fig. 3

¹⁶B. Ya. Gorodilov, I. N. Krupskii, V. G. Manzhelli, and O. A. Korolyuk, *Fiz. Nizk. Temp.* **7**, 424 (1981) [*Sov. J. Low Temp. Phys.* **7**, 208 (1981)]. From Fig. 1.

¹⁷R. G. Bohn and C. F. Mate, *Phys. Rev. B* **2**, 2121 (1970). From Fig. 1.

¹⁸R. G. Bohn (private communication).

¹⁹See P. C. Souers, *Hydrogen Properties for Fusion Energy*, Ref. 6, p. 98. The analysis is based on the Driessen-Silvera equation of state for H₂ and D₂. See A. Driessen, J. A. deWaal, and I. F. Silvera, *J. Low Temp. Phys.* **34**, 255 (1979).

²⁰B. A. Wallace and H. Meyer, *J. Low Temp. Phys.* **15**, 297 (1974).

²¹M. Calkins and H. Meyer, *J. Low Temp. Phys.* **57**, 265 (1984).

²²D. E. Daney, *Cryogenics* **11**, 290 (1971).

²³A. C. Rose-Innes, *Low Temperature Laboratory Techniques* (Crane, Russak, and Co., New York, 1973), pp. 236, 240.

²⁴Reference 6, p. 105.

²⁵ $J=1$ hydrogen is the first excited rotational state, which is metastable for H₂, D₂, and T₂. It must be catalyzed to the ground $J=0$ state. See Ref. 6, pp. 12–13, 308–311.

²⁶Based on our electron paramagnetic resonance experiments, this time dependence is consistent with the time required for the atoms created by the β decay of tritium to reach their "equilibrium" population. The larger defect resistance at lower temperatures also correlates with larger equilibrium atom populations at lower temperatures.

²⁷J. R. Gaines, J. D. Sater, E. M. Fearon, P. C. Souers, F. E. McMurphy, and E. R. Mapoles, *Phys. Rev. B* **37**, 1482 (1988).

²⁸Y. Cao, J. R. Gaines, P. A. Fedders, and P. C. Souers, *Phys. Rev. B* **37**, 1474 (1988).

²⁹R. W. Powers, R. W. Mattox, and H. L. Johnston, *J. Chem. Soc.* **76**, 5972 (1954); **76**, 5974 (1954).

³⁰H. M. Roder and D. E. Diller, *J. Chem. Phys.* **52**, 5928 (1970).

³¹Reference 6, pp. 502–505.

³²W. de Boer, *Nucl. Instrum. Methods* **107**, 99 (1973). Figure 3 has the classic shape of the thermal mixing (dynamic cooling)

curve.

³³W. de Boer, *J. Low Temp. Phys.* **22**, 185 (1976).

³⁴O. S. Leifson and C. D. Jeffries, *Phys. Rev.* **122**, 178 (1961).

³⁵T. J. Schmugge and C. D. Jeffries, *Phys. Rev.* **138**, A1785 (1965). Figures 16 through 18 are classic examples of the solid-state effect.